

## Optical conductivity of the Hubbard model

J. J. Vicente Alvarez and C. A. Balseiro

*Centro Atómico Bariloche and Instituto Balseiro, 8400 Bariloche, República Argentina*

H. A. Ceccatto

*Instituto de Física Rosario, Universidad Nacional de Rosario, Boulevard 27 de Febrero 210 Bis, 2000 Rosario, República Argentina*

(Received 11 September 1996; revised manuscript received 7 February 1997)

We study the response to a static electric field (charge stiffness) and the frequency-dependent conductivity of the Hubbard model in a resonant-valence-bond-type paramagnetic phase. This phase is described by means of a charge and spin rotational-invariant approach, based on a mixed fermion-boson representation of the original strongly correlated electrons. We found that the Mott transition at half filling is well described by the charge stiffness behavior, and that the values for this quantity off half filling agree reasonably well with numerical results. Furthermore, for the frequency-dependent conductivity we trace back to the origin of the band that appears inside the Hubbard gap to magnetic pair breaking. This points to a magnetic origin of the midinfrared band in high- $T_c$  compounds. [S0163-1829(97)01124-7]

### I. INTRODUCTION

In experimental studies of the optical conductivity  $\sigma(\omega)$  in high- $T_c$  materials, it is observed that, upon doping, weight appears inside the charge-transfer gap of the undoped compounds.<sup>1</sup> The origin of this so-called midinfrared band is not completely clear yet, being related for some compounds to trapped holes near dopant atoms, or to the Cu-O chains in the  $\text{YBa}_2\text{Cu}_3\text{O}_{6+x}$  family.<sup>2</sup> On the other hand, numerical studies suggest that the midinfrared band may be caused, at least in part, by the spin excitations that surround hole carriers. Moreover, these studies seem to imply that the unusual behavior of  $\sigma(\omega)$  might be a general feature of strongly interacting electron systems, bearing no connection to the presence of superconductivity.<sup>3</sup>

The two-dimensional single-band Hubbard model is a drastic simplification of realistic multiorbital models proposed to explain the physics of the high- $T_c$  materials. Even so, it contains a great deal of the essential physics of correlated electrons, for which both charge and spin degrees of freedom are relevant. For this reason, most of the numerical studies above mentioned have been performed on this model and its strong-repulsion descendent, the so-called  $t$ - $J$  model.<sup>3</sup> These studies have been carried out on finite lattices of up to  $4 \times 4$  sites, and show clear indications of the appearance of states inside the Hubbard gap. The energy scale of these states should be of the order of the antiferromagnetic coupling  $J \sim 4t^2/U$  to substantiate the claims that they are associated to magnetic fluctuations, but this does not appear so clearly from the numerical results.

Although numerical methods are usually far more reliable than approximate analytical techniques, they suffer from severe limitations related to the small system sizes that can be considered. Consequently, it is of interest to give alternative evidence for the existence of the midinfrared band and to investigate its origin by using less-controlled methods that can access the thermodynamic limit. For the  $t$ - $J$  model, an attempt in this direction<sup>4</sup> found that the inclusion of magnetic fluctuations are essential for these properties. We have re-

cently developed a spin and charge rotational-invariant approach to the Hubbard model,<sup>5,6</sup> based on a mixed fermion-boson representation of the original electrons. It gives a fairly good account of different properties in a paramagnetic phase with only short-range resonantly-valence-band (RVB)-type magnetic correlations, which might correspond to the real situation at  $T=0^+$ . In the present paper, we apply this method to study the static response (Drude weight) and optical conductivity of the Hubbard model, and trace back the origin of the midinfrared band to the interplay between charged bosons and spin fermions used in our description. This confirms the subtle connection of the midinfrared band to magnetic fluctuations, and its appearance as a general feature of strongly correlated electron systems.

In the next section (Sec. II) we introduce the method and set up some notation, in Sec. III we describe the calculation of the Drude weight (or charge stiffness), and in Sec. IV we consider the system response to a homogeneous frequency-dependent electric field and obtain the optical conductivity. Finally, in Sec. V we present some conclusions.

### II. MIXED BOSON-FERMION DESCRIPTION OF CORRELATED ELECTRONS

We consider the Hubbard Hamiltonian,<sup>7</sup>

$$H = -t \sum_{\langle ij \rangle \sigma} c_{i\sigma}^\dagger c_{j\sigma} + U \sum_i \left( n_{i\uparrow} n_{i\downarrow} - \frac{1}{2} n_i \right) - \mu \sum_i n_i, \quad (1)$$

where  $c_{i\sigma}^\dagger$  creates an electron at site  $i$  with spin  $\sigma$ ,  $n_{i\sigma} = c_{i\sigma}^\dagger c_{i\sigma}$ , and  $n_i = n_{i\uparrow} + n_{i\downarrow}$ . We have included an on-site energy  $U/2$  so that the chemical potential  $\mu$  is zero for the half-filled case, and in the following we will measure the energy in units of  $t = 1$ .

As in Ref. 5, we replace the original fermion operators according to  $c_{i\sigma} = e_i^\dagger s_{i\sigma} + \sigma d_i s_{i\sigma}^\dagger$  and the corresponding daggered expressions for their Hermitian conjugates. Here  $e, d$

are bosonic operators associated to the charge degrees of freedom that destroy empty and double occupied sites, respectively. The  $s_\sigma$ 's are fermionic operators that take care of the spin degrees of freedom by destroying single occupied sites with the corresponding spin projection. In order for this to be a faithful representation of the original Fermi algebra, the configuration space must be restricted to have exactly one particle per site, i.e.,  $e_i^\dagger e_i + d_i^\dagger d_i + \sum_\sigma s_{i\sigma}^\dagger s_{i\sigma} = 1$ . This constraint is enforced by introducing Lagrange multipliers  $\lambda_i$  at every site.

In a coherent-state path-integral formulation of the problem we decouple the charge and spin degrees of freedom by means of a Hubbard-Stratonovich transformation. The saddle-point approximation to the resulting path integral is equivalent, for homogeneous Hubbard-Stratonovich fields and  $\lambda$ 's, to a self-consistent diagonalization of the following spin and charge Hamiltonians:

$$H_s = \sum_{\mathbf{k}\sigma} (\epsilon_{\mathbf{k}}^s + \lambda) s_{\mathbf{k}\sigma}^\dagger s_{\mathbf{k}\sigma} - \sum_{\mathbf{k}} g_{\mathbf{k}}^s [s_{\mathbf{k}\uparrow}^\dagger s_{-\mathbf{k}\downarrow}^\dagger + s_{-\mathbf{k}\downarrow} s_{\mathbf{k}\uparrow}], \quad (2)$$

and

$$H_c = \sum_{\mathbf{k}} [(\epsilon_{\mathbf{k}}^e + \lambda) e_{\mathbf{k}}^\dagger e_{\mathbf{k}} + (\epsilon_{\mathbf{k}}^d + \lambda) d_{\mathbf{k}}^\dagger d_{\mathbf{k}}] - \sum_{\mathbf{k}} g_{\mathbf{k}}^c [e_{\mathbf{k}} d_{-\mathbf{k}} + e_{\mathbf{k}}^\dagger d_{-\mathbf{k}}^\dagger]. \quad (3)$$

Here the operators with subindex  $\mathbf{k}$  are the Fourier transform of site operators,  $\epsilon_{\mathbf{k}}^s = -2A\gamma_{\mathbf{k}} - U/2$ ,  $g_{\mathbf{k}}^s = 2B\gamma_{\mathbf{k}}$  for fermions,  $\epsilon_{\mathbf{k}}^e = -2C\gamma_{\mathbf{k}} + \mu$ ,  $\epsilon_{\mathbf{k}}^d = 2C\gamma_{\mathbf{k}} - \mu$ ,  $g_{\mathbf{k}}^c = 2D\gamma_{\mathbf{k}}$  for bosons, and  $\gamma_{\mathbf{k}} = \sum_\alpha \cos k_\alpha$ , with  $k_\alpha$  the  $\alpha$  component of the wave vector  $\mathbf{k}$ . The parameters  $A, B, C$ , and  $D$  are obtained from the self-consistency equations  $A = \langle e_i^\dagger e_j \rangle - \langle d_i^\dagger d_j \rangle$ ,  $B = \langle e_i d_j \rangle + \langle e_j d_i \rangle$ ,  $C = \sum_\sigma \langle s_{i\sigma}^\dagger s_{j\sigma} \rangle$ , and  $D = \langle s_{i\downarrow} s_{j\uparrow} \rangle + \langle s_{j\downarrow} s_{i\uparrow} \rangle$ .

The spin and charge Hamiltonians can be diagonalized by standard Bogoliubov transformations. In the fermionic case we obtain the quasiparticle dispersion relation  $E_{\mathbf{k}}^s = \sqrt{(\epsilon_{\mathbf{k}}^s + \lambda)^2 + (g_{\mathbf{k}}^s)^2}$ . The corresponding result for the charge bosons is  $\omega_{\mathbf{k}}^\pm = E_{\mathbf{k}}^c \pm (\epsilon_{\mathbf{k}}^e - \epsilon_{\mathbf{k}}^d)$ , where  $E_{\mathbf{k}}^c = \sqrt{\lambda^2 - (g_{\mathbf{k}}^c)^2}$ . At half filling  $\mu = 0 = C$ , so that  $\epsilon_{\mathbf{k}}^e = 0 = \epsilon_{\mathbf{k}}^d$  and  $\omega^+ = E_{\mathbf{k}}^c = \omega^-$ . For  $U$  larger than a critical value  $U_c \approx 2.7$  these degenerate bosonic dispersion relations have a gap and the bosons do not condense, which corresponds to the insulating phase. When  $U < U_c$  the gap closes, the bosons condense, and the system becomes a conductor. In this case the ground-state wave function is a mixture of a condensate and paired zero-point excitations:

$$|\Psi_{GS}\rangle = e^{d_0 d_{\mathbf{k}=0}^\dagger + e_0 e_{\mathbf{k}=0}^\dagger - \sum_{\mathbf{k}} b_{\mathbf{k}} e_{\mathbf{k}}^\dagger d_{-\mathbf{k}}^\dagger - \sum_{\mathbf{k}} f_{\mathbf{k}} s_{\mathbf{k}\uparrow}^\dagger s_{-\mathbf{k}\downarrow}^\dagger} |0\rangle. \quad (4)$$

Here  $e_0$  and  $d_0$  are the condensate values and  $b_{\mathbf{k}}, f_{\mathbf{k}}$  can be obtained in terms of the coefficients of the Bogoliubov transformations in the usual way. Notice that in Eq. (4) the zero-point excitations above the condensate are paired, so that they contain the same number of  $e$  and  $d$  and of  $s_\uparrow$  and  $s_\downarrow$  quanta. This is a reflection of the fact that the approximation preserves the rotational and particle-hole symmetries. Off

half filling, however, either the  $\omega^+$  or the  $\omega^-$  branch become gapless, and there is always a condensate with  $e_0 \neq d_0$  that breaks the particle-hole symmetry. Their relative values depend on whether we are doping with particles or holes, and, as expected, the system is always a conductor.

In the next section we will characterize the change in the system behavior (from metallic to insulating) by considering the charge stiffness as a function of doping for  $U > U_c$ .

### III. CHARGE STIFFNESS

Here we examine the current response to a vector potential of wave vector  $\mathbf{q} = 0$  and frequency  $\omega$  in the  $x$  direction,  $A_x(t) = A_x e^{-i\omega t}$ .<sup>8,9</sup> In the presence of the vector potential, the kinetic energy is modified by the Peierls phase factors:  $t \rightarrow t e^{i e x_{ij} A_x(t)}$ , where  $x_{ij} = x_i - x_j = \pm 1$  in units of the lattice spacing. The total current density is  $J_x = ie[P_x, H]$ , with  $P_x = \sum_i x_i n_i$  the polarization operator. Expanding the phase factors to order  $A^2$ , the usual paramagnetic and diamagnetic contributions to the total current are obtained:

$$J_x = e j_x + e^2 T_x A_x. \quad (5)$$

Here  $j_x = it \sum_{\langle ij \rangle} x_{ij} c_{i\sigma}^\dagger c_{j\sigma}$  is the  $x$  component of the paramagnetic current density, and  $T_x = -t \sum_{\langle ij \rangle} x_{ij}^2 c_{i\sigma}^\dagger c_{j\sigma}$  is the kinetic energy associated with the  $x$ -oriented links. The frequency-dependent uniform electric conductivity  $\sigma_{xx}(\omega)$  characterizes the linear response of the current to the electric field  $E_x(\omega) = i\omega A_x(\omega)$ . Its real part is given by

$$\text{Re} \sigma_{xx}(\omega) = 2\pi e^2 \left( \rho_c \delta(\omega) - \frac{1}{2\pi\omega} \text{Im} \Pi_{xx}(\omega + i0^+) \right), \quad (6)$$

where

$$\Pi_{xx}(i\omega_n) = \frac{1}{N} \int_0^\beta d\tau e^{i\omega_n \tau} \langle T_\tau j_x(\tau) j_x(0) \rangle. \quad (7)$$

The Drude weight of the  $\delta$ -function contribution is given in terms of the charge stiffness

$$\rho_c = \frac{1}{2} [\langle -T_x \rangle - \text{Re} \Pi_{xx}(\omega \rightarrow 0)] \quad (8)$$

$$= \frac{1}{N} \left[ \frac{1}{2} \langle -T_x \rangle - \sum_{\nu \neq 0} \frac{|\langle 0 | j_x | \nu \rangle|^2}{E_\nu - E_0} \right], \quad (9)$$

where the last line can be obtained directly from second-order perturbation theory.<sup>8</sup>

By using the slave-boson constraint the polarization operator can be written  $P_x = \sum_i x_i (d_i^\dagger d_i - e_i^\dagger e_i)$ . In this way we assign (opposite) charges only to the bosons, and the paramagnetic current operator becomes

$$j_x = \sum_{\mathbf{k}} [2tC \text{sink}_x(e_{\mathbf{k}}^\dagger e_{\mathbf{k}} - d_{-\mathbf{k}}^\dagger d_{-\mathbf{k}}) + 2tD \text{sink}_x(e_{\mathbf{k}} d_{-\mathbf{k}} + e_{\mathbf{k}}^\dagger d_{-\mathbf{k}}^\dagger)]. \quad (10)$$

This procedure is arbitrary and reflects the gauge invariance introduced in the theory by splitting the original fermion operators.<sup>10</sup> Using this freedom one can transfer the effects

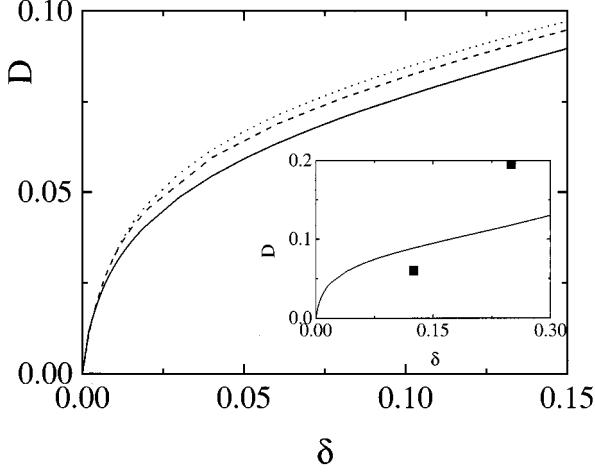


FIG. 1. Charge stiffness  $\rho_c$  as a function of doping for  $U=6$  (full line), 8 (dashed line), and 10 (point line). Inset: Comparison of our result for  $U=8$  with numerical results on a  $4 \times 4$  lattice from Ref. 3.

of the Peierls phase factor entirely to the bosons, which is physically motivated by their interpretation as charge operators.

The evaluation of Eqs. (9) and (10) shows that the paired zero-point excitations give no contribution to the charge stiffness, which could be expected, since the pairs do not carry charge. The charge boson condensate contributes only to the kinetic energy, so that the stiffness becomes

$$\rho_c = tC(e_0^2 - d_0^2) + 2tDe_0d_0. \quad (11)$$

In Fig. 1 we show the behavior of  $\rho_c$  as a function of doping for different values of  $U$ . The inset gives a comparison to exact numerical results for the charge stiffness obtained on a  $4 \times 4$  lattice at  $U=8$ .<sup>3</sup> Notice that the extrapolation to half filling of the numerical results would give a negative stiffness, which is related to the small size of the lattice and explains in part the small discrepancies with our result. The same qualitative behavior is obtained for all values of  $U$  ( $U > U_c$ ). As expected,  $\rho_c$  is zero in the insulating phase ( $\delta=0$ ), the onset of conductivity occurs at zero doping and has a steep rise for small doping that becomes more pronounced as we increase  $U$ . This is in agreement with numerical results, and is related to the decreasing of the RVB singlet binding energy with  $U$  in our picture (which is analogous to the decreasing of  $J$  in the short-range antiferromagnetic phase of the  $t-J$  model).

In the next section we will discuss the system's response to a frequency-dependent applied field.

#### IV. OPTICAL CONDUCTIVITY

The response of the system to a time-varying applied field is given by the optical conductivity (6). To study the current-current response function  $\Pi_{xx}(\omega + i0^+)$  entering in this expression, we consider the current operator in terms of the original fermions:  $j_{x,q=0} = it \sum_{i\sigma} (c_{i\sigma}^\dagger c_{i+x\sigma} - c_{i+x\sigma}^\dagger c_{i\sigma})$ , and replace them by the slave fermions and bosons. In a factor-

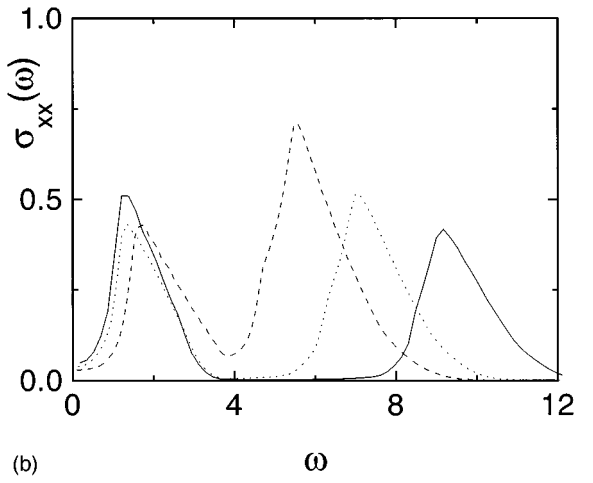
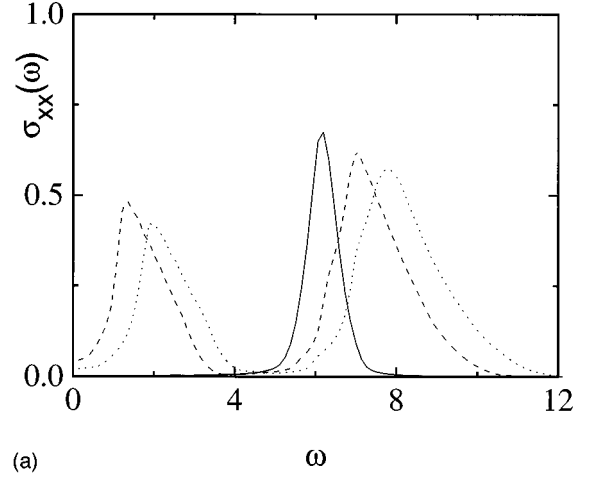


FIG. 2. Optical conductivity  $\sigma_{xx}(\omega)$  as a function of  $\omega$  for (a)  $U=6$  and  $\delta=0$  (full line), 0.1 (dashed line), and 0.2 (point line); (b)  $\delta=0.1$  and  $U=4$  (dashed line), 6 (point line), and 8 (full line).

ized form convenient for further manipulations, the final result is

$$j_{x,q=0} = \frac{1}{N} \sum_{\mathbf{q}} \sum_{s=\pm} s \sum_{\alpha=1}^4 \left( \sum_{\mathbf{k}'} \phi_{\mathbf{k}'-}^\dagger B_{s,\alpha}(\mathbf{k}'-, \mathbf{k}'_+) \phi_{\mathbf{k}'_+} \right) \times \left( \sum_{\mathbf{k}} \psi_{\mathbf{k}-}^\dagger F_{-s,\alpha}(\mathbf{k}_-, \mathbf{k}_+) \psi_{\mathbf{k}_+} \right), \quad (12)$$

where  $\mathbf{k}_\pm = \mathbf{k} \pm \mathbf{q}/2$ ,  $\phi_{\mathbf{k}}^\dagger = (e_{\mathbf{k}}^\dagger, d_{-\mathbf{k}})$ , and  $\psi_{\mathbf{k}}^\dagger = (s_{\mathbf{k}\uparrow}^\dagger, s_{-\mathbf{k}\downarrow})$ . The  $2 \times 2$  matrices  $B_{s,\alpha}$  and  $F_{s,\alpha}$  are defined as

$$B_{s,1}(\mathbf{k}_-, \mathbf{k}_+) = \frac{1}{2} \begin{pmatrix} \epsilon_{\mathbf{k}_-}^s & 0 \\ 0 & \epsilon_{-\mathbf{k}_+}^s \end{pmatrix},$$

$$B_{s,3}(\mathbf{k}_-, \mathbf{k}_+) = \frac{1}{2} \begin{pmatrix} 0 & -\epsilon_{-\mathbf{k}_+}^s \\ 0 & 0 \end{pmatrix}, \quad (13)$$

$$F_{s,3}(\mathbf{k}_+, \mathbf{k}_-) = \frac{1}{2} \begin{pmatrix} 0 & 0 \\ \epsilon_{\mathbf{k}_-}^s + \epsilon_{-\mathbf{k}_+}^s & 0 \end{pmatrix}, \quad (14)$$

where  $\epsilon_{\mathbf{k}}^+ = \cos k_x$ ,  $\epsilon_{\mathbf{k}}^- = \sin k_x$ , and  $B_{s,2}(\mathbf{k}_-, \mathbf{k}_+) = B_{s,1}(\mathbf{k}_+, \mathbf{k}_-)$ ,  $B_{s,4}(\mathbf{k}_-, \mathbf{k}_+) = B_{s,3}^t(\mathbf{k}_+, \mathbf{k}_-)$ ,  $F_{s,i}(\mathbf{k}_+, \mathbf{k}_-) = B_{s,i}(\mathbf{k}_-, \mathbf{k}_+)$  ( $i=1,2$ ), and  $F_{s,4}(\mathbf{k}_+, \mathbf{k}_-) = F_{s,3}^t(\mathbf{k}_-, \mathbf{k}_+)$ .

Note that this expression for the current would lead to the same result for the charge stiffness than the simpler one [Eq. (10)] used in the calculation of the previous section. This is so because for a static electric field the paired chargeless fermions are not excited by the field (the Drude weight is due only to the contribution of the condensed bosons). However,

for a dynamic field they contribute through their interactions with the zero-point bosonic excitations. In particular, Eq. (12) reduces to Eq. (10) by simply taking its ground-state average in the fermionic spin sector.

The dynamical part of the conductivity can now be obtained from Eqs. (6) and (7) by a direct calculation of the time-ordered products of fermions and bosons. At the saddle-point level the result is a convolution of fermion and boson susceptibilities, which can be split into two contributions:  $\sigma(\omega) = \sigma_1(\omega) + \sigma_2(\omega)$ . We found

$$\begin{aligned} \sigma_1(\omega) = & \sum_{\mathbf{q}} \sum_{r,s=\pm} rs \sum_{\alpha,\beta=1}^4 \{ \text{Tr}[D^0 B_{r,\alpha}(0,\mathbf{q}) D_{\mathbf{q}}^- B_{s,\beta}(\mathbf{q},0)] \text{Tr}[G_{\mathbf{k}_+}^+ F_{-r,\alpha}(\mathbf{k}_+, \mathbf{k}_-) G_{\mathbf{k}_-}^- F_{-s,\beta}(\mathbf{k}_-, \mathbf{k}_+)] \\ & \times \delta[\omega^2 - (\omega_{\mathbf{q}}^- + E_{\mathbf{k}_+} + E_{\mathbf{k}_-})^2] - \text{Tr}[D^0 B_{r,\alpha}(0,\mathbf{q}) D_{\mathbf{q}}^+ B_{s,\beta}(\mathbf{q},0)] \text{Tr}[G_{\mathbf{k}_+}^- F_{-r,\alpha}(\mathbf{k}_+, \mathbf{k}_-) G_{\mathbf{k}_-}^+ F_{-s,\beta}(\mathbf{k}_-, \mathbf{k}_+)] \\ & \times \delta[\omega^2 - (\omega_{\mathbf{q}}^+ + E_{\mathbf{k}_+} + E_{\mathbf{k}_-})^2] \} \end{aligned}$$

and

$$\begin{aligned} \sigma_2(\omega) = & \sum_{\mathbf{q}} \sum_{r,s=\pm} rs \sum_{\alpha,\beta=1}^4 \{ \text{Tr}[D_{\mathbf{k}_+}^+ B_{r,\alpha}(\mathbf{k}_+, \mathbf{k}_-) D_{\mathbf{k}_-}^- B_{s,\beta}(\mathbf{k}_-, \mathbf{k}_+)] \text{Tr}[G_{\mathbf{k}_-}^+ F_{-r,\alpha}(\mathbf{k}_-, \mathbf{k}_+) G_{\mathbf{k}_+}^- F_{-s,\beta}(\mathbf{k}_+, \mathbf{k}_-)] \\ & \times \delta[\omega^2 - (\omega_{\mathbf{k}_+}^+ + \omega_{\mathbf{k}_-}^- + E_{\mathbf{k}_+} + E_{\mathbf{k}_-})^2] \}. \end{aligned}$$

Here

$$D^0 = \begin{pmatrix} e_0^2 & e_0 d_0 \\ e_0 d_0 & d_0^2 \end{pmatrix}$$

and we introduced the bosonic propagator  $D_{\mathbf{k}}(i\omega) = D_{\mathbf{k}}^+/(i\omega - \omega_{\mathbf{k}}^+) + D_{\mathbf{k}}^-/(i\omega + \omega_{\mathbf{k}}^-)$ , which is the Fourier transform of  $D_{\mathbf{k}}(\tau) = -\langle T_{\tau} \phi_{\mathbf{k}}(\tau) \phi_{\mathbf{k}}^{\dagger}(0) \rangle$ , and the corresponding fermionic propagator  $G_{\mathbf{k}}(i\omega) = G_{\mathbf{k}}^+/(i\omega + E_{\mathbf{k}}) + G_{\mathbf{k}}^-/(i\omega - E_{\mathbf{k}})$ . The term  $\sigma_1(\omega)$  corresponds to the contribution of the condensate and zero-point excitation products, while  $\sigma_2(\omega)$  comes from the paired-paired excitation terms.

In Fig. 2 we present the results for the optical conductivity with  $\omega > 0$ . In Fig. 2(a) we show  $\sigma_{xx}(\omega)$  for  $U=6$  and different values of  $\delta$ . The contributions of the low-energy excitations characteristic of the metallic behavior are contained in the Drude peak (not shown in this figure), which has a total weight given in Fig. 1. It can be seen that upon doping a well-developed midinfrared band appears. At a frequency  $\omega \sim U$  the excitations involving the upper Hubbard band give a second peak in  $\sigma_{xx}(\omega)$ . The integrated area of the midinfrared band is comparable to the upper Hubbard band, this is in agreement with numerical results.<sup>3</sup> As  $\delta$  increases the chemical potential moves down and, as expected, the upper Hubbard band contribution to the conductivity moves to higher frequencies. Note that the same behavior is obtained for the midinfrared band. In Fig. 2(b) we give  $\sigma_{xx}(\omega)$  for  $\delta=0.1$  and different values of  $U$ . In this case, while the contribution of the upper Hubbard band moves to higher energies, the midinfrared band moves toward the origin with increasing  $U$ . This result could be taken

as an indirect evidence that the midinfrared band is associated with the spin excitations that have a characteristic energy scale given by  $J$  and decreases with increasing  $U$ . The upper Hubbard band is clearly associated with double occupancy excitations. More precisely, the contribution  $\sigma_1$  to the optical conductivity mentioned above can be split in two terms that involve the breaking of two spin singlet pairs, with the energies of these processes shifted by those of the ‘‘acoustic’’ (gapless) and ‘‘optical’’ (gapped) boson branches, respectively. The transitions that contribute to the weight inside the Hubbard gap are associated to the term with the acoustic branch, so that the energies involved near  $\mathbf{k}=0$  correspond only to magnetic pair breaking. The second term contributes to the upper Hubbard band along with the processes involved in  $\sigma_2$  (two spin pair-breaking processes plus the creation of both acoustical and optical boson excitations).

In closing this section, we would like to comment on the sum rule fulfilled by the optical conductivity, which relates the frequency integral of  $\sigma_{xx}(\omega)$  to the mean kinetic energy. In our case, the results do not satisfy this condition due to the unphysical enlargement of the Fock space inherent to the kind of approximation we are using. This has been recognized in previous studies of other properties, such as the one-particle spectral density and momentum-space occupation number.<sup>11</sup> The sum rule for the frequency-dependent conductivity is given by<sup>8</sup>

$$\frac{1}{2\pi e^2} \int_{-\infty}^{\infty} d\omega \sigma_{xx}(\omega) = -\frac{\langle T_x \rangle}{2}. \quad (15)$$

To fulfill this relation the kinetic energy has to be calculated in the same approximation as  $\sigma_{xx}(\omega)$ , which in our calculation scheme goes beyond the saddle-point level.

In order to get an idea of the magnitude of the deviation in the sum rule, we have calculated Eq. (15) for the half-filled case using the kinetic energy corrected by Gaussian fluctuations.<sup>13</sup> In this case we found a disagreement of about 15% between the right-hand and left-hand side terms of Eq. (15). To show that for doped systems the deviation is of the same order, an explicit calculation of  $\langle T_x \rangle$  beyond the saddle-point level is required. Such calculation is not available and is out of the scope of the present paper. We stress that using the Gaussian fluctuations for the kinetic energy is only a way to estimate the left-hand side of Eq. (15) but does not guarantee that the two terms of the sum rule have been calculated at the same footness. A cure to these problems results from a proper handling of the particle-number restriction in constrained Hamiltonian theory,<sup>12</sup> which is, however, out of the scope of the present paper.

## V. CONCLUSIONS

We have performed a study of the linear response of the Hubbard model to a homogeneous electric field, by using a mixed boson-fermion representation of the original strongly correlated electrons. In a paramagnetic phase of the RVB type, with only short-range spin singlets, the system presents a Mott transition that can be characterized by the behavior of the charge stiffness  $\rho_c$ , i.e., the response to a static field. In particular, the values of  $\rho_c$  as a function of doping for large  $U$  was found to agree reasonably well with numerical results,

and to steeply vanish when approaching the insulating phase at half filling. Moreover, its behavior with increasing  $U$  (slightly rising with  $U$ ) follows the pattern observed in numerical studies.

The saddle-point approximation used to calculate the frequency-dependent conductivity allows us to separate the charge and spin degrees of freedom that in our description are of bosonic and fermionic character, respectively. The real electron excitations are to be calculated as a convolution of these two contributions. In the large  $U$  limit studied in this work, the half-filled case is insulating. Only upon doping, the system becomes metallic and is signed by the occurrence of a Drude peak. In this phase the charge excitations have two branches, an acoustic and an optical one; the later involves double occupation and has a characteristic energy of the order of  $U$ . The spin excitations have a single gapped branch, these excitations correspond to break RVB-type singlets. The electron-hole type excitations induced by the external field involve charge and spin excitations. In the limit of uniform electric field ( $q \rightarrow 0$ ) the acoustic charge branch convoluted with the spin excitations give rise to the midinfrared absorption, the optical charge branch always involves double occupation and contributes to the upper band.

In conclusion the frequency-dependent conductivity shows a well developed midinfrared band, which we related to the pair-breaking of RVB singlets. This connection highlights the importance of magnetic processes in the appearance of weight inside the Hubbard gap, and points to the presence of a midinfrared band as a generic feature of Hubbard and  $t$ - $J$ -like models, and perhaps of most strongly correlated electron systems.

<sup>1</sup>T. Timusk and D. B. Tanner (unpublished); D. B. Tanner and T. Timusk (unpublished).

<sup>2</sup>G. A. Thomas *et al.*, Phys. Rev. B **45**, 2474 (1992); Z. Schlesinger *et al.*, Phys. Rev. Lett. **65**, 801 (1990).

<sup>3</sup>Elbio Dagotto, Rev. Mod. Phys. **66**, 763 (1994).

<sup>4</sup>Y. M. Li, D. N. Sheng, Z. B. Su, and L. Yu, Mod. Phys. Lett. B **5**, 1467 (1991).

<sup>5</sup>J. J. Vicente Alvarez, C. A. Balseiro, and H. A. Ceccatto, Phys. Rev. B **54**, 11 207 (1996).

<sup>6</sup>J. J. Vicente Alvarez, H. A. Ceccatto, and C. A. Balseiro, Phys. Rev. B **52**, 14 511 (1995).

<sup>7</sup>J. Hubbard, Proc. R. Soc. London, Ser. A **276**, 238 (1963).

<sup>8</sup>B. Shastry and B. Sutherland, Phys. Rev. Lett. **65**, 243 (1990).

<sup>9</sup>D. J. Scalapino, S. R. White, and S. C. Zhang, Phys. Rev. Lett. **68**, 2830 (1992).

<sup>10</sup>Z. Zou and P. W. Anderson, Phys. Rev. B **37**, 627 (1988).

<sup>11</sup>Shiping Feng, J. B. Wu, Z. B. Su, and L. Yu, Phys. Rev. B **47**, 15 192 (1993).

<sup>12</sup>J. C. Le Guillou and E. Ragoucy, Phys. Rev. B **52**, 2403 (1995).

<sup>13</sup>J. J. Vicente Alvarez, Ph.D. thesis, Universidad Nac. de Cuyo Instituto Balseiro, 1997.